Two-chain spin ladder with frustrating second-neighbor interactions

Zheng Weihong,* V. Kotov,† and J. Oitmaa‡
School of Physics, The University of New South Wales, Sydney, NSW 2052, Australia
(Received 31 October 1997)

The Heisenberg model on a two-chain spin-$\frac{1}{2}$ ladder with frustrating second-neighbor interactions is studied by using series expansions about the Ising and dimer limits, numerical diagonalization, and by Abelian bosonization analysis. The phase diagram is determined, and pair correlations and the complete dispersion relations for the triplet spin-wave excitations are also computed. [S0163-1829(98)11617-X]

I. INTRODUCTION

Heisenberg spin ladders have been the subject of intense theoretical and experimental research in recent years. It is by now well established that single chain Heisenberg antiferromagnets with integer spin have a gap in the excitation spectrum, whereas those with half-integer spin have gapless excitations. The former have a finite correlation length, while for the latter it is infinite with the spin-spin correlation function decaying as a power law. For $S=\frac{1}{2}$ Heisenberg spin ladders,[1–3] the systems with an even number of legs have an energy gap, short-range correlations, and a ''spin-liquid'' ground state. On the other hand, the systems with odd number of legs have gapless excitations, quasi-long-range order, and a power-law falloff of spin-spin correlations, similar to single chains.

In this paper, we study the Heisenberg model on a two-chain ladder with second-neighbor interactions, via Ising and dimer expansions, diagonalization of finite systems, and Abelian bosonization. All of the work is at $T=0$. The motivation for studying such a system is twofold. First we wish to explore the effect of frustration on the properties of two-leg $s=\frac{1}{2}$ ladders. Weak frustration is not expected to change the physics of the gapped system qualitatively. However strong frustration may change the nature of the ground state at some critical coupling ratio, corresponding to a $T=0$ phase transition. Furthermore in other systems, such as the J_1-J_2 chain, frustration itself leads to the creation of a gapped dimer phase, and thus in the present case there is the possibility of observing the competition between two independent gap yielding perturbations. The second reason for studying such a generalized ladder system is the possibility that in real two-leg ladder materials significant second-neighbor interactions will be present.

We write the Hamiltonian of our system as

$$H(J_\parallel,J_\perp,J_2)=\sum_i [J_\parallel(\mathbf{S}_{1,i}\cdot\mathbf{S}_{1,i+1}+\mathbf{S}_{2,i}\cdot\mathbf{S}_{2,i+1})+J_\perp\mathbf{S}_{1,i}\cdot\mathbf{S}_{2,i} + J_2(\mathbf{S}_{1,i}\cdot\mathbf{S}_{2,i+1}+\mathbf{S}_{2,i}\cdot\mathbf{S}_{1,i+1})], \quad (1)$$

where $\mathbf{S}_{l,i}$ denotes the $S=1/2$ spin at site i of the lth chain. $J_\parallel$ is the interaction between nearest-neighbor spins along the chain, $J_\perp$ is the interactions between nearest-neighbor spins along the rungs, J_2 is the interactions between the second-neighbor spins. This is shown in Fig. 1(a). We denote the ratio of couplings as $y_1\equiv J_\perp/J_\parallel$ and $y_2\equiv J_2/J_\parallel$. In the present paper all couplings are taken to be antiferromagnetic (that is, $J_\parallel$, $J_\perp$, $J_2>0$).

The system has an interesting symmetry property: If one exchanges the couplings $J_\parallel$ and J_2, one can recover the original Hamiltonian by exchanging two spins along the rungs at even sites, that is, the Hamiltonian will be invariant under exchanging the couplings $J_\parallel$ and J_2:

$$H(J_\parallel,J_\perp,J_2)=H(J_2,J_\perp,J_\parallel). \quad (2)$$

Therefore we only need to study the case of $y_2\leqslant 1$, and the system with $y_2>1$ can be mapped into system with $y_2\leqslant 1$ through the identity in Eq. (2).

There has been some previous work on this system. Of course for $J_2=0$ we recover the usual two-leg ladders,[1–3] which has gapless excitations only when $J_\perp=0$. The case $y_2=1$ has special properties. Bose and Gayen[4] pointed out that this system has an exact dimer state: a state in which

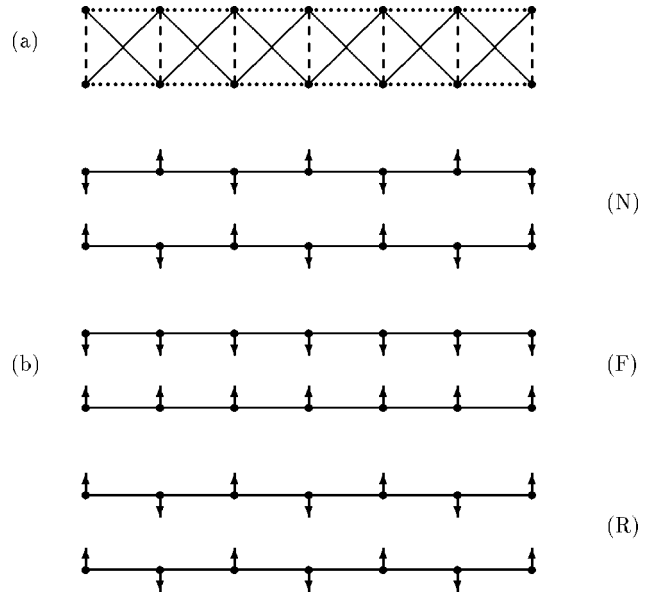

FIG. 1. (a) Three different couplings considered: $J_\parallel$ (the dotted lines), $J_\perp$ (the dashed lines), and J_2 (the solid lines). (b) Three different spin orders for the system at the Ising limit: the Néel state (N), the ferromagnetic chain state (F), and the ferromagnetic rung state (R).

 © 1998 The American Physical Society

every pair of spins along the rungs form a singlet, and this perfect dimer state is the ground state for large enough values of y_1. Xian[5] performed a systematic study of this system via a microscopic approach based on a proper set of composite operators, and found that the Hamiltonian consists of two commuting parts:

$$H=\sum_i J_\perp \mathbf{S}_{1,i}\cdot\mathbf{S}_{2,i}+J_\parallel \mathbf{P}_i\cdot\mathbf{P}_{i+1}, \tag{3}$$

where $\mathbf{P}_i$ represents the effective spin-1 operator at site i. The first part, $J_\perp \mathbf{S}_{1,i}\cdot\mathbf{S}_{2,i}$, is trivial, with no interaction between different rungs and with a gap $J_\perp$ between the singlet and triplet states. The second part, $J_\parallel \mathbf{P}_i\cdot\mathbf{P}_{i+1}$, is similar to the spin-1 Heisenberg chain with each rung in the ladder corresponding to each site in the spin-1 chain. Because the two parts of H commute it follows that there is an eigenstate of H with eigenvalue:

$$E_g=(J_\parallel e_0+J_\perp/4)N/2, \tag{4}$$

where $e_0=-1.401\,484\,038\,97(4)$ is the ground-state energy per site of the spin-1 Heisenberg chain.[6] The eigenvalue for the state with singlets on all of the rungs is

$$E_g=(-3J_\perp/4)N/2. \tag{5}$$

Therefore one can easily determine the transition point $y_c=1.401\,484\,038\,97(4)$. At this crossing point the singlet-singlet gap is zero. Kitatani and Oguchi[7] had independently considered the existence of a state of singlet dimers for this system for $y_2=1$, and had obtained the same results as above.

This paper studies the general case where exact results are not known. In Sec. II we report results obtained by Ising and dimer expansions at $T=0$. We compute the ground-state energy and the complete spin-wave excitation spectra, as well as obtaining more accurate estimates for various quantities for the simple case $J_2=0$. We also carry out finite-lattice diagonalization studies for systems of 16 and 24 spins, paying particular attention to the behavior of spin-spin correlations. Section III describes an analytic approach, based on Abelian bosonization. When comparisons are possible the various methods all provide a consistent picture. Finally in Sec. IV we provide a summary and draw some conclusions.

II. NUMERICAL RESULTS

We report here the results of numerical studies, using both series expansions and diagonalizations. These methods provide results over the whole phase diagram, and give the most detailed picture of the behavior of this system for general values of the couplings. Our previous series work on the ladder system[3] used expansions about both the Ising limit and about a fully dimerized state, and we refer to that paper and references therein for technical details.

A. Ising expansions

To construct an expansion about the Ising limit for this system, one has to introduce an anisotropy parameter x, and write the Hamiltonian as

$$H=H_0+xV, \tag{6}$$

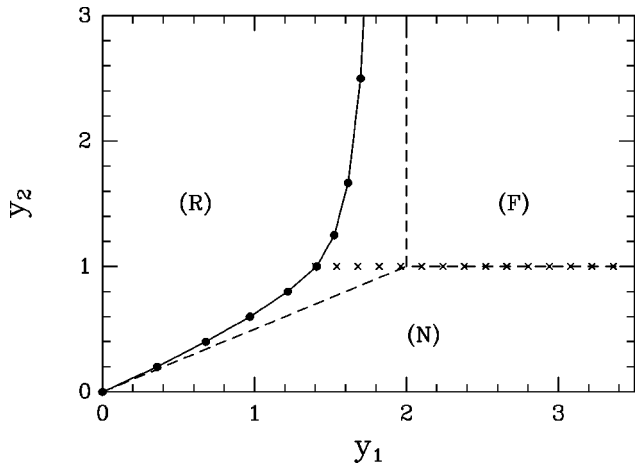

FIG. 2. Phase diagram in the (y_1,y_2) plane. The dashed lines show the phase boundary for the three different spin orders of the system at the Ising limit. The solid line shows the phase boundary between the dimerized phase (right side) and Haldane-type phase (left side) for the isotropic system. Along this line there is a vanishing singlet-singlet gap. The ''×'' line ($y_2=1$, $y_1\geqslant 1.401\,484$) is the location of the exact dimer ground states.

where

$$H_0=\sum_i [J_\parallel(S^z_{1,i}S^z_{1,i+1}+S^z_{2,i}S^z_{2,i+1})+J_\perp S^z_{1,i}S^z_{2,i} + J_2(S^z_{1,i}S^z_{2,i+1}+S^z_{2,i}S^z_{1,i+1})], \tag{7a}$$

$$V=\sum_i [J_\parallel(S^x_{1,i}S^x_{1,i+1}+S^y_{1,i}S^y_{1,i+1}+S^x_{2,i}S^x_{2,i+1}+S^y_{2,i}S^y_{2,i+1}) + J_\perp(S^x_{1,i}S^x_{2,i}+S^y_{1,i}S^y_{2,i}) + J_2(S^x_{1,i}S^x_{2,i+1}+S^y_{1,i}S^y_{2,i+1}+S^x_{2,i}S^x_{1,i+1}+S^y_{2,i}S^y_{1,i+1})]. \tag{7b}$$

The limits $x=0$ and $x=1$ correspond, respectively, to the Ising and isotropic Heisenberg limit, the latter being the case of primary interest.

Since H_0 is taken as the unperturbed Hamiltonian we need to identify the ground states. There are three of these, shown in Fig. 1(b). We refer to these as the Néel state (N), the ferromagnetic chain state (F), and the ferromagnetic rung state (R). Their regions of stability are indicated in Fig. 2. The line $y_2=1$, $y_1\geqslant 2$ is a boundary between N and F states. The operator V is treated as a perturbation: it flips pairs of spins on neighboring sites. The quantum fluctuations represented by V will of course result in much more complex ground states. Since the system is effectively one-dimensional no true long-range order can exist, even at $T=0$.

As in our earlier paper,[3] to overcome a possible singularity at $x<1$, and to get a better convergent series in the Heisenberg limit, we add to the Hamiltonian the following staggered field term:

$$\Delta H = t(1-x)\sum_{i,l} (-1)^{i+l} S^z_{l,i} \tag{8}$$

for the expansion about the Néel state, or the following field term:

$$\Delta H = t(1-x)\sum_{i,l} (-1)^{i} S^z_{l,i} \tag{9}$$

for the expansion about the ferromagnetic rung state. ΔH vanishes at the isotropic limit $x=1$. We adjust the coefficient t to get the most smooth terms in the series, with a typical value being $t=2$.

The series-expansion method has been previously described in several articles,[8–10] and will not be repeated here. We have developed Ising expansions about both the Néel and ferromagnetic rung states for the ground-state energy per site E_0/N and the triplet spin-wave excitation spectrum for different ratios of couplings y_1 and y_2 and (simultaneously) for several values of t up to order x^{13}. The resulting series are available on request. These series have been analyzed by using integrated first-order inhomogeneous differential approximants and Padé approximants.[11] We will discuss these results later in this section.

B. Dimer expansions

In the limit that the exchange coupling along the rungs $J_\perp$ is much larger than the couplings $J_\parallel$ and J_2, the rungs interact only weakly with each other, and the dominant configuration in the ground state is the product state with the spins on each rung forming a spin singlet. The Hamiltonian in Eq. (1) can then be rewritten as

$$H/J_\perp = H_0 + (1/y_1)V, \tag{10}$$

where

$$H_0 = \sum_i \mathbf{S}_{1,i}\cdot\mathbf{S}_{2,i},$$

$$V = \sum_i [(\mathbf{S}_{1,i}\cdot\mathbf{S}_{1,i+1} + \mathbf{S}_{2,i}\cdot\mathbf{S}_{2,i+1}) + y_2(\mathbf{S}_{1,i}\cdot\mathbf{S}_{2,i+1} + \mathbf{S}_{2,i}\cdot\mathbf{S}_{1,i+1})]. \tag{11}$$

We can obtain an expansion in $(1/y_1)$ by treating the operator H_0 as the unperturbed Hamiltonian, and the operator V as a perturbation.

We have carried out the dimer expansions for the ground-state energy up to order $(1/y_1)^{23}$ and for the triplet excitation spectrum up to order $(1/y_1)^{13}$ for different values of y_2. The resulting series for some particular values of y_2 are listed in Table I. The rest of the series are available on request. In our previous paper,[3] the series for the case $y_2=0$ were computed up to order $(1/y_1)^9$ for the ground-state energy and up to order $(1/y_1)^8$ for the triplet excitation spectrum. Our present results agree with and considerably extend these previous results. Again, we use integrated first-order inhomogeneous differential approximants and Padé approximants[11] to extrapolate the series.

The ground-state energy per site E_0/N is shown in Fig. 3, where curves for $y_2=0,0.2,0.4,0.6,0.8,1$ are shown as functions of $y_1=J_\perp/J_\parallel$. The curves (connecting the full point symbols) emanating from the left side (small y_1) are obtained from Ising expansion about the R state. Those emanating from the right side are from the dimer expansion. The estimates from the Ising expansion about the N state agree very well with these and are not shown separately (except for the case of $y_2=0$ which are shown by open point symbols with error bars). These curves, for any given y_2, cross at a transition point y_{1c}. This corresponds to a first-order ground-state phase transition, resulting from a level crossing. The numerical estimate for $y_2=1$ of $y_{1c}=1.40$ is in good agreement with the exact result of Xian[5] and Kitatani and Oguchi[7] discussed above. The locus of the transition points is shown in Fig. 2, and represents a ''gapless line'' where the gap between the two lowest energies, both of which are singlets, vanishes. Everywhere else the ground state is a nondegenerate singlet. However this is not a gapless line in the usual sense of a vanishing gap for elementary excitations.

There are two branches of triplet spin excitations which we denote $\epsilon_g(k)$, $\epsilon_u(k)$ corresponding to symmetric and antisymmetric states with respect to interchange of the two chains. k is the wave number along the chain direction. On the left side of the gapless line in Fig. 2, which can be called a ''Haldane'' phase, these two branches are independent and each has the appearance of a simple cosine dispersion curve, symmetric about $k=\pi/2$ and having a finite gap at the minimum energy points. However on the right side of the gapless line, the ''dimerized region,'' the branches are no longer independent, being related by

$$\epsilon_g(k) = \epsilon_u(\pi - k) \tag{12}$$

and having a complex form, without the symmetry about $k=\pi/2$ found in the Haldane region. This relation can be understood as follows. Consider an initial down spin at site j flipped to create an excitation. To form a Bloch state this excitation will couple to other downs spins. In the Néel or small y_2 region this involves even sites on the upper chain and odd sites on the lower chain leading to a shift of π in the wave number. The dispersion curves are shown in Figs. 4 and 5 for $y_1=1$ for particular values of y_2. The triplet gap appears to be nonzero throughout the phase diagram, except at $y_1=y_2=0$.

Since the dimer expansion carried out here is much longer than our previous calculations,[3] we can make more accurate estimates for the normal two-leg ladder without frustration $(J_2=0)$. The ground-state energy is estimated to be

$$E_0/(NJ_\parallel) = -0.578\,043(2) \quad \text{at } J_\parallel = J_\perp. \tag{13}$$

In Fig. 6 we show the dependence of the triplet excitation gap $\epsilon_u(\pi)$ on $J_\perp/(J_\perp+J_\parallel)$, in particular, they are estimated to be

$$\epsilon_u(\pi)/J_\parallel = 0.5028(8) \quad \text{at } J_\parallel = J_\perp; \tag{14}$$

$$\epsilon_u(\pi)/J_\perp = 0.405(15) \quad \text{at } J_\parallel \gg J_\perp. \tag{15}$$

These results agree very well with the recent quantum Monte Carlo results of Frischmuth *et al.*[12] and Greven, Birgeneau, and Wiese.[2]

TABLE I. Series coefficients for the dimer expansion of the ground-state energy per site $E_0/(NJ_\perp)$, and the energy gap $\epsilon_u(\pi)/J_\perp$. Coefficients of y_1^{-n} are listed for $y_2=0,0.2,0.4,0.6,0.8$.

n	$y_2=0$	$y_2=0.2$	$y_2=0.4$	$y_2=0.6$	$y_2=0.8$
			Ground-state energy $E_0/(NJ_\perp)$		
0	$-3.750000000\times10^{-1}$	$-3.750000000\times10^{-1}$	$-3.750000000\times10^{-1}$	$-3.750000000\times10^{-1}$	$-3.750000000\times10^{-1}$
1	0.000000000	0.000000000	0.000000000	0.000000000	0.000000000
2	$-1.875000000\times10^{-1}$	$-1.200000000\times10^{-1}$	$-6.750000000\times10^{-2}$	$-3.000000000\times10^{-2}$	$-7.500000000\times10^{-3}$
3	$-9.375000000\times10^{-2}$	$-7.200000000\times10^{-2}$	$-4.725000000\times10^{-2}$	$-2.400000000\times10^{-2}$	$-6.750000000\times10^{-3}$
4	1.171875000×10^{-2}	$-1.920000000\times10^{-2}$	$-2.548125000\times10^{-2}$	$-1.770000000\times10^{-2}$	$-5.981250000\times10^{-3}$
5	8.789062500×10^{-2}	2.880000000×10^{-2}	$-2.953125000\times10^{-3}$	$-1.080000000\times10^{-2}$	$-5.146875000\times10^{-3}$
6	7.763671875×10^{-2}	4.771200000×10^{-2}	1.317346875×10^{-2}	$-4.452000000\times10^{-3}$	$-4.292531250\times10^{-3}$
7	$-2.682495117\times10^{-2}$	2.536560000×10^{-2}	1.777094648×10^{-2}	3.552000000×10^{-4}	$-3.463308984\times10^{-3}$
8	$-1.381530762\times10^{-1}$	$-2.345664000\times10^{-2}$	1.045650727×10^{-2}	3.014910000×10^{-3}	$-2.699781797\times10^{-3}$
9	$-1.184420586\times10^{-1}$	$-5.932056600\times10^{-2}$	$-3.351507699\times10^{-3}$	3.491262000×10^{-3}	$-2.033702734\times10^{-3}$
10	8.023428917×10^{-2}	$-4.401953880\times10^{-2}$	$-1.476726810\times10^{-2}$	2.292678800×10^{-3}	$-1.486153249\times10^{-3}$
11	2.926602935×10^{-1}	2.352668756×10^{-2}	$-1.616860920\times10^{-2}$	2.872863433×10^{-4}	$-1.066983590\times10^{-3}$
12	2.174702423×10^{-1}	9.158584993×10^{-2}	$-5.942062903\times10^{-3}$	$-1.585372406\times10^{-3}$	$-7.754224757\times10^{-4}$
13	$-2.513295675\times10^{-1}$	8.611973765×10^{-2}	9.811790575×10^{-3}	$-2.607764454\times10^{-3}$	$-6.016035581\times10^{-4}$
14	$-7.079677824\times10^{-1}$	$-2.062191934\times10^{-2}$	2.034441425×10^{-2}	$-2.487025970\times10^{-3}$	$-5.287392850\times10^{-4}$
15	$-4.220720468\times10^{-1}$	$-1.567438679\times10^{-1}$	1.702026317×10^{-2}	$-1.402179099\times10^{-3}$	$-5.356521930\times10^{-4}$
16	8.048506089×10^{-1}	$-1.794371390\times10^{-1}$	$-1.145012657\times10^{-4}$	1.136830590×10^{-4}	$-5.993625741\times10^{-4}$
17	1.836906814	1.631560655×10^{-4}	$-2.064904725\times10^{-2}$	1.407604936×10^{-3}	$-6.974813639\times10^{-4}$
18	7.873287228×10^{-1}	2.827706741×10^{-1}	$-2.936191639\times10^{-2}$	1.968009179×10^{-3}	$-8.101904773\times10^{-4}$
19	-2.609038806	3.876215459×10^{-1}	$-1.667240377\times10^{-2}$	1.615756127×10^{-3}	$-9.216722624\times10^{-4}$
20	-4.952285110	7.857208468×10^{-2}	1.260776202×10^{-2}	5.560918471×10^{-4}	$-1.020922924\times10^{-3}$
21	-1.190569396	$-5.222477673\times10^{-1}$	3.933197151×10^{-2}	$-7.233155669\times10^{-4}$	$-1.101950155\times10^{-3}$
22	8.511630761	$-8.553338679\times10^{-1}$	4.125471073×10^{-2}	$-1.663509824\times10^{-3}$	$-1.163436744\times10^{-3}$
23	1.360832756×10^{1}	$-3.290829443\times10^{-1}$	9.852975277×10^{-3}	$-1.867815929\times10^{-3}$	$-1.207975395\times10^{-3}$
			Energy gap $\epsilon_u(\pi)/J_\perp$		
0	1.000000000	1.000000000	1.000000000	1.000000000	1.000000000
1	-1.000000000	$-8.000000000\times10^{-1}$	$-6.000000000\times10^{-1}$	$-4.000000000\times10^{-1}$	$-2.000000000\times10^{-1}$
2	5.000000000×10^{-1}	3.200000000×10^{-1}	1.800000000×10^{-1}	8.000000000×10^{-2}	2.000000000×10^{-2}
3	2.500000000×10^{-1}	1.600000000×10^{-1}	9.000000000×10^{-2}	4.000000000×10^{-2}	1.000000000×10^{-2}
4	$-1.250000000\times10^{-1}$	$-6.080000000\times10^{-2}$	$-3.780000000\times10^{-2}$	$-2.480000000\times10^{-2}$	$-9.800000000\times10^{-3}$
5	$-2.734375000\times10^{-1}$	$-1.596800000\times10^{-1}$	$-1.098225000\times10^{-1}$	$-7.624000000\times10^{-2}$	$-3.200750000\times10^{-2}$
6	$-1.533203125\times10^{-1}$	$-1.282880000\times10^{-1}$	$-1.210798125\times10^{-1}$	$-1.114720000\times10^{-1}$	$-5.737081250\times10^{-2}$
7	2.456054688×10^{-1}	5.984960000×10^{-2}	$-4.939160625\times10^{-2}$	$-1.189328000\times10^{-1}$	$-8.546363125\times10^{-2}$
8	4.813385010×10^{-1}	2.335137600×10^{-1}	5.900339848×10^{-2}	$-9.919344000\times10^{-2}$	$-1.162613828\times10^{-1}$
9	1.322269440×10^{-1}	2.147366880×10^{-1}	1.432105375×10^{-1}	$-5.701525600\times10^{-2}$	$-1.496337233\times10^{-1}$
10	$-6.962262789\times10^{-1}$	$-7.397652400\times10^{-2}$	1.363951349×10^{-1}	$-5.152148667\times10^{-3}$	$-1.855936645\times10^{-1}$
11	-1.056785534	$-4.262824117\times10^{-1}$	2.673760586×10^{-2}	4.221120509×10^{-2}	$-2.241092352\times10^{-1}$
12	5.050360756×10^{-2}	$-4.592008720\times10^{-1}$	$-1.317976096\times10^{-1}$	7.169697802×10^{-2}	$-2.651208173\times10^{-1}$
13	2.122963428	6.458482125×10^{-2}	$-2.320399129\times10^{-1}$	7.586016636×10^{-2}	$-3.084074357\times10^{-1}$

C. Exact diagonalizations

In order to obtain a more complete picture of the energy spectrum, the correct assignment of spin quantum number S to different levels, and the variation of spin-spin correlations throughout the phase diagram, we have carried out exact Lanczos diagonalizations for ladders with $N=16$ and $N=24$ spins. The finite-lattice corrections appear to be quite small and the results are believed to be representative of the thermodynamic limit.

In Fig. 7 we show the energies of low-lying energies for $N=24$, for a scan through the phase diagram (Fig. 2) at $y_2=0.8$. The solid lines represent singlets ($S=0$), while triplet levels ($S=1$) are shown as dashed lines. The existence of the transition point discussed above, the finite singlet-triplet gap, and other level crossings can be seen. There is a region around the transition point where the lowest triplet lies above the lowest two singlets. The location of the transition point, while less accurately resolvable, is totally consistent with the series results given above. In Fig. 8 we show some pair correlations for the same scan through the phase diagram at $y_2=0.8$. The correlations show large discontinuities at the transition point $y_1\simeq1.24$. The sign of various correlations is consistent with ferromagnetic rung (R)-type order for $y_1<1.24$ and Néel-type order for $y_1>1.24$, in accordance with the

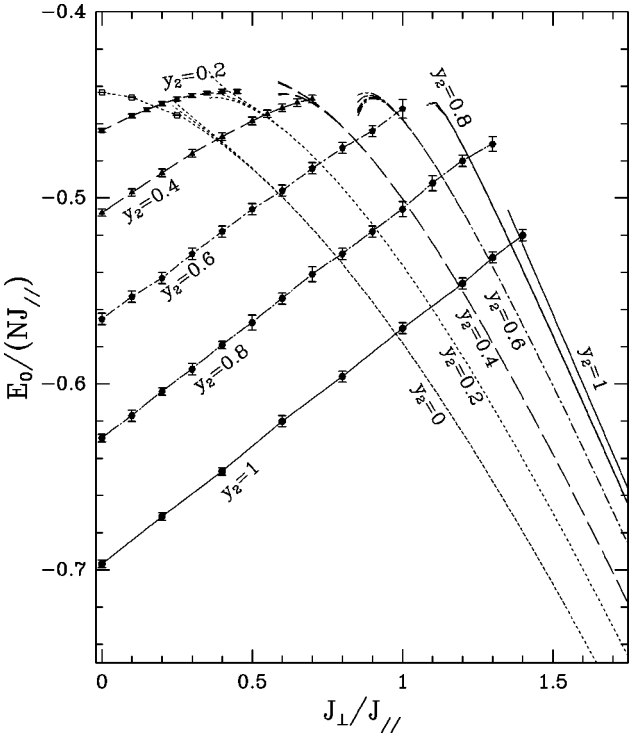

FIG. 3. The ground-state energy per site $E_0/(NJ_\parallel)$ as a function of $y_1=J_\perp/J_\parallel$ for $y_2=0,0.2,0.4,0.6,0.8,1$. The lines in the large y_1 region are the extrapolations of integrated differential approximants to the dimer series, the full point symbols connected by a line are estimates from Ising expansions about the ferromagnetic rung state, and the open point symbols (for $y_2=0$ only) are estimates from Ising expansions about the Néel state. The position of crossing indicates a transition point with vanishing singlet-singlet gap.

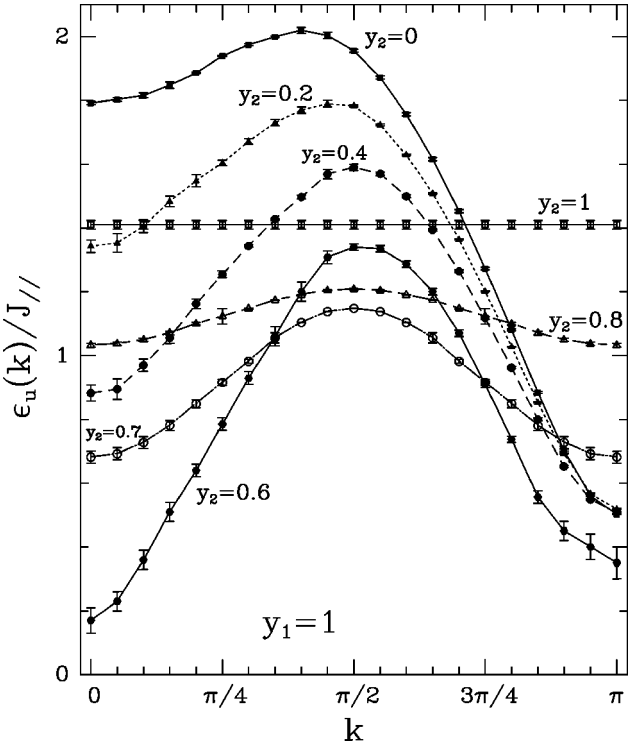

FIG. 4. The dispersions $\epsilon_u(k)$ of the spin-triplet excited states of the two-chain ladder with interchain coupling $y_1=1$ and $y_2=0,0.2,0.4,0.6,0.7,0.8,1$. The results for $y_2<0.6$ are estimated from the dimer expansions, and results for $y_2\geqslant 0.6$ are estimated from the Ising expansions about the ferromagnetic rung order.

classical ground states in Fig. 1. We note also that further-neighbor correlations become very small for increasing y_1, consistent with a dimerized phase.

III. WEAK-COUPLING ANALYSIS

In this section we present analysis, based on Abelian bosonization, which can determine the phase boundary between the ferromagnetic rung (Haldane-type) and Néel ground states. Our considerations are valid in the limit of small $J_\perp$ and J_2. Since the procedure is well described in the literature,[13–15] we will give only the basic steps here.

The spin operators for each chain are transformed, by using the Jordan-Wigner transformation, into a system of spinless fermions a_n (chain 1) and b_n (chain 2) at half filling. Next, since we are interested in the low-energy properties of the model, we pass to a continuum description, which was developed for a single chain by Luther and Peschel.[13] The spectrum of the Jordan-Wigner fermions is linearized in the vicinity of the two Fermi points $\pm k_F=\pm\pi/2$:

$$a_n=\sqrt{a}[e^{ik_Fn}\psi_{1R}(x=na)+e^{-ik_Fn}\psi_{1L}(x=na)], \quad (16)$$

where a is the lattice spacing, and ψ_{1R}, ψ_{1L} are slowly varying on the scale of the lattice. An analogous transformation is applied to the second chain (with corresponding fields ψ_{2R}, ψ_{2L}). In order to write the ladder Hamiltonian (1) in bosonic form, we make use of the Abelian bosonization rules:

$$\psi_{1R,1L}=\frac{1}{\sqrt{2\pi\alpha}}\exp[\pm i\sqrt{4\pi}\phi_{1R,1L}(x)], \quad (17)$$

where $\alpha^{-1}\sim a^{-1}$ is a large momentum cutoff, and

$$\phi_{1R,1L}(x)=\frac{1}{2}[\phi_1(x)\pm\theta_1(x)]. \quad (18)$$

Here $\theta_1(x)$ is defined as the field, dual to $\phi_1(x)$, i.e., $\partial_x\theta_1(x)=\Pi_1(x)$, and $\Pi_1(x)$ is the momentum field, conjugate to $\phi_1(x)$. Similar equations describe the second chain. Using the above formulas the interchain interactions can be bosonized, with the result

$$H=\sum_{s=+,-}\frac{v_s}{2}\int dx\left[\frac{1}{K_s}(\partial_x\phi_s)^2+K_s(\partial_x\theta_s)^2\right]+\tilde{H}, \quad (19)$$

$$\tilde{H}=\frac{C}{\alpha^2}\int dx[g_1\cos(\sqrt{8\pi}\phi_+)+g_2\cos(\sqrt{8\pi}\phi_-) +2g_3\cos(\sqrt{2\pi}\theta_-)]. \quad (20)$$

In the above equations, the symmetric and antisymmetric combinations of the fields are introduced via $\sqrt{2}\phi_\pm=\phi_1\pm\phi_2$, and similarly for the dual fields. The (bare) values of the coupling constants in Eq. (20) are $g_i=y_1-2y_2, i=1,2,3$, and C is a cutoff independent constant. The Luttinger-liquid parameters in Eq. (19) depend on the bare couplings:

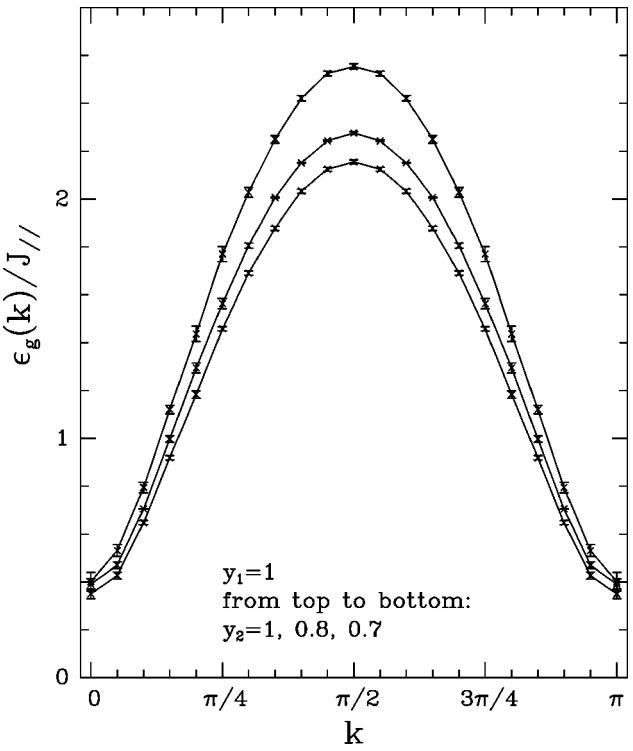

FIG. 5. The dispersions $\epsilon_g(k)$ of the spin-triplet excited states of the two-chain ladder with interchain coupling $y_1=1$ and $y_2=1,0.8,0.7$ (shown in the figure from the top to the bottom, respectively). The results are estimated from the Ising expansion about the ferromagnetic rung order.

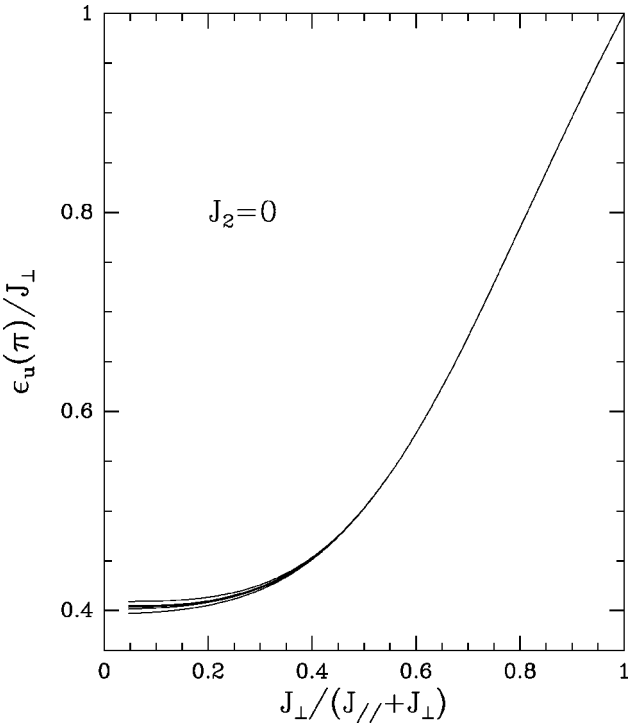

FIG. 6. The minimum triplet energy gap $\epsilon_u(\pi)/J_\parallel$ for the system with $J_2=0$ as a function of $J_\perp/(J_\perp+J_\parallel)$. The results are estimated from the several different integrated differential approximants to the dimer series.

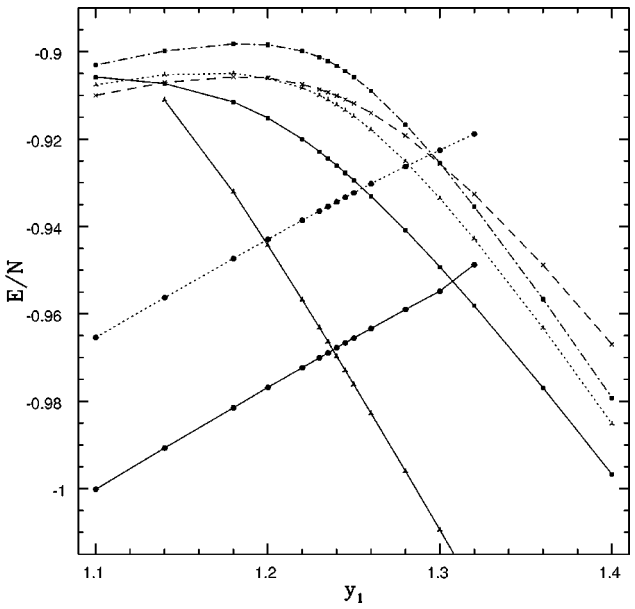

FIG. 7. Low-lying energies for a system of $N=24$ spins, for fixed $y_2=0.8$. Solid (dashed) lines represent singlet (triplet) levels, respectively.

$$v_\pm = 1 + \frac{\delta}{\pi} \pm \frac{y_1 + 2y_2}{2\pi} + \text{higher order}, \tag{21}$$

$$K_\pm = 1 - 2\frac{\delta}{\pi} \mp \frac{y_1 + 2y_2}{2\pi} + \text{higher order}. \tag{22}$$

Without the y_2 terms our equations are similar to the ones obtained by Strong and Millis for the simple ladder.[15] In order to emphasize that the second terms in Eqs. (21) and (22) come from the Ising interactions in the two chains, we have introduced the anisotropy parameter δ (i.e., $J_\parallel^z \to J_\parallel \delta$,

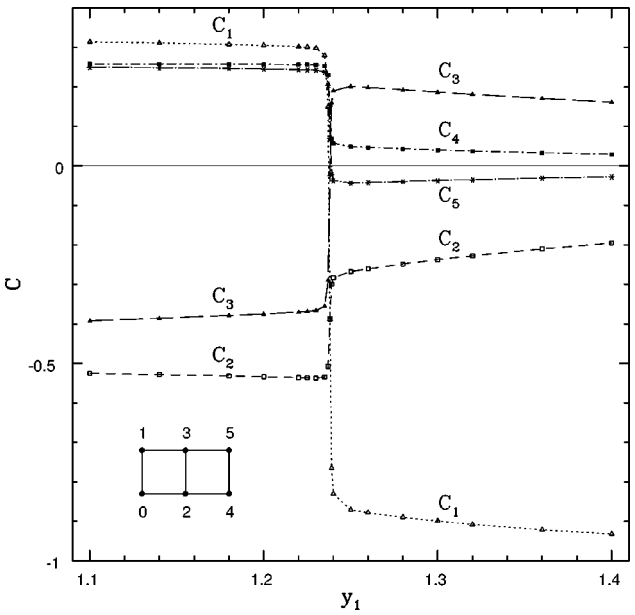

FIG. 8. Pair correlations $C_n = 4\langle S_0^z S_n^z \rangle$ in the ground state for $N=24$ at fixed $y_2=0.8$. Note the discontinuities in correlations at the transition points $y_{1c} \simeq 1.24$ (which decrease slightly as the lattice size N increases).

and we should set $\delta=1$ at the isotropic point). In the limit $y_1, y_2 \to 0$ the exact form of the above functions are known from the Bethe ansatz solution of the chain problem, and, in particular for $\delta=1$ we have $v_\pm=\pi/2$, $K_\pm=1/2$.[13] Away from this exactly solvable limit, expressions (21) and (22) should be viewed as valid only to lowest order in δ, y_1, and y_2, since all lattice renormalization effects have been neglected in passing to the continuum limit. We have displayed in Eq. (20) only the relevant [in renormalization-group (RG) sense[14]] operators and have neglected all potentially irrelevant and marginal ones. The latter contain terms that mix the symmetric and antisymmetric sectors, as well as combinations of field derivatives and cosines.

The scaling dimensions of the three cosine operators in Eq. (20) are $2K_+$, $2K_-$, and $(2K_-)^{-1}$ (corresponding to g_1, g_2, and g_3, respectively). A cosine operators is relevant if its scaling dimension is less than two. Thus, in the limit $y_1=y_2=0$, all operators have dimension one and are relevant. For nonzero values of the interchain couplings, one can easily see that the most relevant operators are g_1 and g_3. These two couplings thus flow to infinity which signals formation of a gap. This strong-coupling regime corresponds to a nonzero expectation value of $\langle \vec{S}_1 \cdot \vec{S}_2 \rangle$.[15] Whether a ferromagnetic rung (Haldane) or antiferromagnetic ladder (Néel) state is realized, depends on the sign of g_1 and g_3. The equations, governing the RG flow for g_1 and g_3 are the usual Kosterlitz-Thouless equations.[15] Thus, if initially $g_1(0), g_3(0)>0$, then $g_1(l), g_3(l) \to \infty$, where l is the RG iteration parameter. This is the Néel state, characterized by a gap to triplet excitations. In the opposite limit $g_1(0), g_3(0)<0$ the couplings flow to minus infinity, which is interpreted as a ladder with an effective ferromagnetic interchain coupling. Thus we conclude that the transition line between the two states is given by the equation $g_1=g_3=y_1-2y_2=0$.

Let us note that as y_1 and y_2 increase one should include higher-order terms in the operator product expansion, which leads to Eq. (20). The additional terms are still less relevant than the ones in Eq. (20) but they typically couple the symmetric and antisymmetric sectors. Thus, the renormalization of g_1 affects g_3 and vice versa. The location of the transition line, however, is not affected by this coupling. On the other hand, we expect that lattice renormalization effects, i.e., inclusion of higher-order terms in the lattice spacing, might lead to a change of the shape of the transition line, as suggested by numerical simulations (see Fig. 2).

IV. CONCLUSIONS

We have studied the two-chain antiferromagnetic spin ladder with frustrating second-neighbor interactions, using a variety of numerical and analytic methods. When the interchain nearest-neighbor coupling $J_\perp$ is dominant the system is in a gapped ''dimerized phase,'' whereas for dominant second-neighbor coupling J_2 the system is in a gapped ''Haldane'' phase, which can be mapped onto an $S=1$ chain. These phases have the same physical origin within the low-energy field theoretic framework but are distinguished by different behavior of correlations and are separated by a first-order transition line where there is a vanishing singlet-singlet gap. The system has a trivial ''valence-bond-solid'' ground state along a line in the phase diagram which separates two types of classical Ising ground state. A symmetry of the Hamiltonian allows these states to be mapped onto each other.

Using series expansions, about both Ising and dimerized unperturbed states, we have computed the ground-state energy and dispersion curves for singlet-triplet excitations. The latter show a qualitative change in form as the second-neighbor interaction changes. Our series in dimer expansions are substantially longer than in our previous study for $J_2=0$, and we obtain very accurate estimates for the ground state and excitation gap, which agree very well with recent quantum Monte Carlo results. We have also computed ground-state energies and correlations using exact diagonalizations for $N=16$, 24. These give a further physical of the nature of the ground state in different regions of phase diagram.

Finally we present an analytical study, valid for small $J_\perp$ and J_2, using the technique of Abelian bosonization. This gives a picture consistent with the numerical work.

ACKNOWLEDGMENT

This work forms part of a research project supported by a grant from the Australian Research Council.

*Electronic address: w.zheng@unsw.edu.au
†Electronic address: vnk@newt.phys.unsw.edu.au
‡Electronic address: otja@newt.phys.unsw.edu.au

[1] E. Dagotto and T.M. Rice, Science **271**, 618 (1996).
[2] M. Greven, R.J. Birgeneau, and U.J. Wiese, Phys. Rev. Lett. **77**, 1865 (1996).
[3] J. Oitmaa, R.R.P. Singh, and W.H. Zheng, Phys. Rev. B **54**, 1009 (1996).
[4] I. Bose and S. Gayen, Phys. Rev. B **48**, 10 653 (1993).
[5] Y. Xian, Phys. Rev. B **52**, 12 485 (1995).
[6] S.R. White and D.A. Huse, Phys. Rev. B **48**, 3844 (1993).
[7] H. Kitatani and T. Oguchi, J. Phys. Soc. Jpn. **65**, 1387 (1996).
[8] H.X. He, C.J. Hamer, and J. Oitmaa, J. Phys. A **23**, 1775 (1990).
[9] M.P. Gelfand, R.R.P. Singh, and D.A. Huse, J. Stat. Phys. **59**, 1093 (1990).
[10] M.P. Gelfand, Solid State Commun. **98**, 11 (1996).
[11] A.J. Guttmann, in *Phase Transitions and Critical Phenomena*, edited by C. Domb and M.S. Green (Academic, New York, 1989), Vol. 13.
[12] B. Frischmuth, B. Ammon, and M. Troyer, Phys. Rev. B **54**, R3714 (1996).
[13] A. Luther and I. Peschel, Phys. Rev. B **9**, 2911 (1974).
[14] H.J. Schulz, Phys. Rev. B **34**, 6372 (1986).
[15] S.P. Strong and A.J. Millis, Phys. Rev. B **50**, 9911 (1994).